Effects of ultrasound on polymeric foam porosity

C. Torres-Sanchez *, J.R. Corney

School of Engineering and Physical Sciences, Mechanical Engineering, Heriot-Watt University, Edinburgh EH14 4AS, UK

Received 12 November 2006; received in revised form 17 April 2007; accepted 8 May 2007

Abstract

A variety of materials require functionally graded cellular microstructures whose porosity is engineered to meet specific applications (e.g. mimic bone structure for orthopaedic applications; fulfil mechanical, thermal or acoustic constraints in structural foamed components, etc.). Although a huge variety of foams can be manufactured with homogenous porosity, there are no generic processes for controlling the distribution of porosity within the resulting matrix.

Motivated by the desire to create a flexible process for engineering heterogeneous foams, the authors have investigated how ultrasound, applied during the formation of a polyurethane foam, affects its cellular structure. The experimental results demonstrated how the parameters of ultrasound exposure (i.e. frequency and applied power) influenced the volume and distribution of pores within the final polyurethane matrix: the data demonstrates that porosity (i.e. volume fraction) varies in direct proportion to both the acoustic pressure and frequency of the ultrasound signal.

The effects of ultrasound on porosity demonstrated by this work offer the prospect of a manufacturing process that can adjust the cellular geometry of foam and hence ensure that the resulting characteristics match the functional requirements.

1. Introduction

If the local porosity of foamed materials could be controlled, then the density and structure of many manufactured components could be designed to achieve optimum performance. Such a manufacturing technology would be particularly useful in bio-mimetics applications where it is frequently observed that biological micro-structures require inhomogeneous morphologies to achieve particular functional, or structural, properties [1,2]. Consequently, the ability to control porosity would enable a variety of biomedical applications, ranging from the development of biological scaffolds to improved filtration, and drug release devices [2,3]. The structure of a foam is characterised by the distribution, size and wall thickness of cells in the bulk material. These features are the result of many factors (e.g. temperature, pressure, reactants concentrations, etc.) some of which are known to be affected by ultrasonic irradiation. Nearly all manufactured foams have homogeneous cellular structures to ensure uniform mechanical properties, so although the need for heterogeneous cellular materials has been widely recognised [4–6], there are few viable manufacturing processes for production of such materials [7].

The aim of the work reported here is to investigate the feasibility of varying the structure of cellular foams through precisely measured and localised application of ultrasound at critical points during the foaming process. The effects investigated are illustrated in Fig. 1, which shows a cross-section of two foams: homogeneous foam created with no irradiation (Fig. 1a), and heterogeneous foam generated under the presence of ultrasound (Fig. 1b).

This paper is structured as follows: Section 2 outlines chemical and ultrasonic principles underlying the sonochemistry process described. Section 3 introduces the

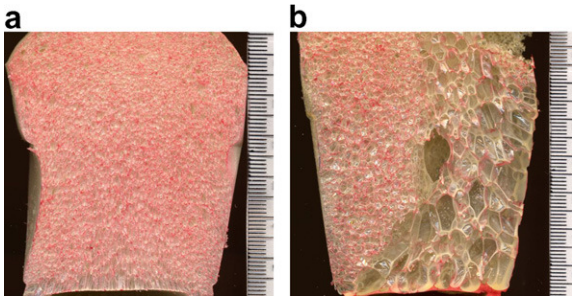

Fig. 1a and 1b. Polymeric foams generated without and with ultrasonic irradiation, respectively.

experimental procedure. Section 4 presents the results and Section 5 discusses the wider significance of the findings before some conclusions are drawn in Section 6.

2. Background

2.1. Polymeric foams

Foam is the dispersion of a gas in a liquid, which creates a characteristic structure when the matrix solidifies. Once cured, the foam consists of individual cells, or pores, the walls of which have completely polymerised and solidified to form a skeletal structure. Polyurethane cells can be open with interconnected cells having a thin membrane between the skeletal ribs, or closed with separate cells which are non permeable and resistant to moisture and oil, insulating against heat and cold and absorbent of impacts or vibrations. A typical foaming reaction [8] involves four stages: 1. bubble generation (nucleation) and growth (often involving a blowing agent); 2. packing of the bubble network and cell window stabilization (cross-linking of polymeric chains); 3. polymer stiffening and, if a flexible foam, cell opening; and 4. final curing (solidification)

The resulting foam structure is affected by both their chemical composition (e.g. blowing agents, surfactants and catalysts) and processing conditions (e.g. pressure, temperature, cure time, humidity, impurities, etc.). The foam used in this study is created by a chemical reaction between polyols and diisocyanate group to produce polyurethane [9,10] with distilled water employed as a blowing agent. The chemical reaction that occurs is:

$$\mathrm{HO{-}R{-}OH\,(\mathbf{polyol}) + O{=}C{=}N{-}R'{-}N{=}C{=}O\,(\mathbf{diisocyanate\ group})} \rightarrow \mathrm{{-}O{-}R{-}O{-}CO{-}NH{-}R'{-}NH{-}CO{-}\,(\mathbf{PU}) + CO_2}$$

The water diffuses between the chains of polyurethane (**PU**) reacting at the same time with the isocyanate groups at the end of the chains, causing the reticulation, or cross-linking, of the polymer, and forming a semi-rigid solid.

2.2. Sonochemistry

In the context of sonochemistry for foams, the literature [11–15] reports applications that control polymerisation rate, enable defoaming in bottling of fizzy drinks and the dissipation of foam in reaction/fermentation vessels. The majority of these applications exploit ultrasonically stimulated transient cavitation effects: the rapid growth and explosive collapse of microscopic bubbles as the alternate compression and rarefaction phases of a sound wave passes through the liquid.

Another well-known effect of ultrasound in polymer chemistry is the non-random depolymerisation of chains in solution [11]. Polymerisation reactions occur with statistical probabilities so that a sample will contain chains with varying lengths and molecular weights. The polymer properties depend critically on both the average molecular weight and the distribution of chain lengths, or polydispersity. Consequently, ultrasound can be used to control these parameters during polymerisation reactions [12].

The ability of ultrasound to modify diffusivity and membrane permeability has been known for decades (essentially, cavitation effects perturb cell membrane structures and increases their permeability) and it is now an established technology for food dehydration and drug delivery [16,17]. These sonication effects should influence both bubble growth and nucleation rates in foams since both are strongly influenced by the concentration of dissolved gas in the resin (in other words the saturation level determines the gas pressure and hence the driving force for bubble growth). Indeed, nucleation of bubbles has been reported to be substantially enhanced by ultrasonic excitation as a means of mechanical activation. The ultrasonic excitation is employed to locally introduce sufficient energy to overcome the energy barrier for bubble nucleation [13].

Once initiated, ultrasound could effect the process of bubble growth in a number of ways [18]:

1. *Heating and mixing*. Increases in temperature, due to absorption of the sound waves, can provoke convections and turbulences that stirs the mixture and reduces the effective viscosity.
2. *Structural effects.* Dynamic agitation, and the shear stresses produced, can affect structural properties (e.g. viscosity) and provoke mechanical rupture.
3. *Cyclic compression and rarefaction.* The acoustic field will subject the bubble to alternate cycles of compression and expansion. When the bubble pulsates for many cycles, this so called 'stable cavitation' enhances the bubble growth. But when the bubble overexcites, 'transient cavitation' occurs causing collapse of the bubbles. The rate depends on the frequency and intensity of the ultrasonic wave.

Although theoretical studies of the behaviour of a single bubble exposed to ultrasound have been reported, the behaviour of whole matrixes of growing bubbles (i.e. a foaming process) do not appear to have been explicitly modelled, but theoretical analysis has lead researchers [19] to identify two possible cavitational behaviours.

When a gas is dissolved in a liquid, changes in pressure and temperature can cause the liquid to become supersatu-

rated and so bubbles are formed. When these bubbles, of initial small radii, are irradiated, they suffer alternate expansion/contraction due to the sinusoidal nature of the soundwave field. Under conditions of *stable cavitation*, this process is positive, and expansions are bigger than contractions, so the bubble growth is in resonance with the soundwave. However, if the bubble size, the ultrasound power and/or frequency go above a certain threshold, *cavitation becomes transient*. The bubble is no longer in resonance and the pressure produced during the next compression cycle causes the bubble to implode.

But while such bubble dynamics play an important role, other processes also enhanced by ultrasound (i.e. diffusion and mixing) will also influence the dynamics of the process of foam formation.

Particularly important in the context of foams and other high viscosity fluids is the ability of ultrasound to produce an increase in mass transport due to diffusion variation [20]. Essentially, sound affects the viscosity of fluids significantly (usually decreasing their viscosity), so acoustic radiation reduces the diffusion boundary layer, increases the concentration gradient and may increase the diffusion coefficient. Since viscosity is inversely proportional to the diffusion coefficient, the latter will increase in sound fields. Turbulent convection also decreases the thickness of the mass transfer boundary layer, i.e. the wall of the pore. An increase in the membrane transport is due to reduced wall thickness. In addition, ultrasound creates stresses that disrupt the normal configuration (shape, wall thickness) of pores, and thus increases the membrane permeability towards gas/vapour, blowing agent. However, if the shear forces provoked by ultrasound are excessive, some cells might rupture affecting the viscoelastic equilibrium in the matrix and, in extreme conditions, leading to foam collapse.

The authors conjectured that it should be possible to modify the behaviour of foaming processes with careful application of ultrasound and as a direct consequence alter the cellular structure (i.e. porosity) of the resulting material. The next section details the experimental work carried out to investigate this hypothesis and establish the relative importance of the different mechanisms acting on the polymeric irradiated system.

3. Experimental investigation

To enable a systematic investigation of the effect of ultrasound on the formation and final porosity of polyurethane foam, samples were irradiated in a temperature controlled water bath over a range of low frequencies and powers. The following sections detail the arrangement of ultrasonic sources/receivers within the water bath and the chemical reactants used.

3.1. Apparatus

The schematic shown in Fig. 2a and 2b illustrates the relative location of the ultrasonic source and the polypropylene container (material chosen for its similar acoustic impedance to water) that held the reactants (5 cm diameter, 7 cm height, 0.16 mm thickness) within the 4 l ($30 \times 15 \times 15$ cm) water bath (lined to minimise ultrasonic reflection). The container was firmly clamped with a lab stand and positioned along the longitudinal axis of the bath. The ultrasonic piezoelectric sources used (a Bandelin Sonopuls sonotrode, Germany, UW 3200) irradiated at 20 kHz, and (a Coltène/Whaledent, USA, BioSonic US100) irradiated at 25 and 30 kHz. The applied power from the transducer varied depending on the experimental series and more details can be found in Section 4. In order to have both transducer and receiver aligned, the sonotrode tip was immersed 2 cm below the free surface, on the same plane that central plane of the container, 5 cm away from the right wall and placed in a central location (7.5 cm from the long sidewalls).

The use of water bath ensured the temperature of the environment could be controlled independently of the effects of ultrasound. The bath temperature was set at 313 K and controlled within ± 1 K. Water was chosen as coupling agent for ultrasound to transmit inside the bath

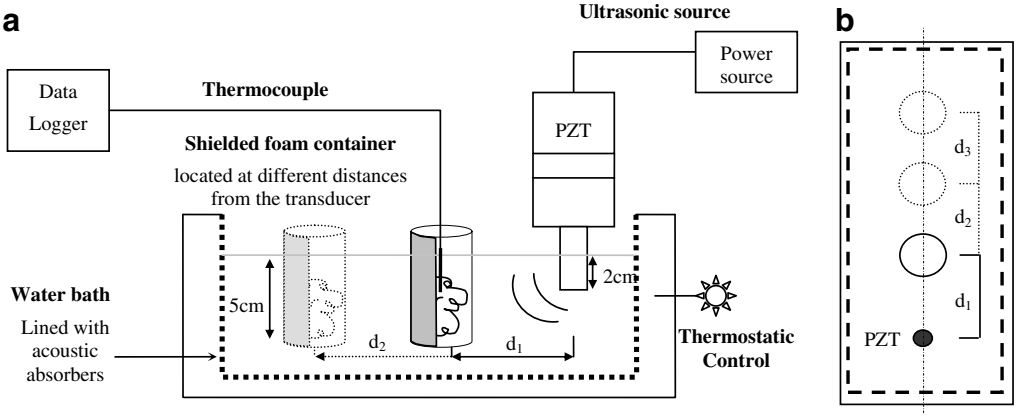

Fig. 2a and 2b. Schematic of the experimental rig, lateral and plan views.

from the ultrasonic probe to the containers and because of its high specific heat. Thermocouples were held in the middle of the mixture and used to monitor the reaction and establish its completion (i.e. after peak temperature).

3.1.1. Experimental chemicals

The polymers used in this study (Dow Europe GmbH, Switzerland) were degassed from the blowing agent (i.e. methane, ether, isobutane) by dissolving in pure acetone. The polyurethane forming reaction was initialised by the addition of distilled water, which started a two stage process described in [10]. In the first stage, the water diffused into the system across the polyurethane chains causing the reticulation of the polymer and dissolving the acetone. In the second stage, the diffusion of acetone in water, which occupied the holes, or spaces, between the reticulated polymer took place. In all cases, the diisocyanate content in the mixture was rectified to have a fixed 40%, and the amount of distilled water added was directly related to that amount (20 vol% H_2O per ml mixture). Both solution and distilled water were kept at a controlled temperature to minimise organic solvent evaporation. The relation PU–acetone used was 50/50 vol%. The mixture containing polyols, isocyanate and solvent was mixed with the chemical blowing agent (i.e. distilled water) using the same procedure of stirring at a standard time of 70 s and minimising air intake into the mixture.

All mixtures were sonicated in an open-vessel container to avoid the build up of the internal pressure due to the water vapour and gases (e.g. CO_2) generated by the reaction that could provoke unwanted implosion of bubbles. Containers faced perpendicularly the sonicating probe and had the opposite 180° of their surface shielded by absorbent material to minimise reflections from the walls and enable investigation of the effects by ''direct'' sonication. During the polymer foaming, the sonication conditions were of 'far field' (i.e. pressure waves that are combined to form a more uniform front that the one in the 'near field' [21]).

3.1.2. Method

The foams were irradiated with ultrasound for 20 min in an off/on cycle of 2 min on/1 min off starting after adding the distilled water, and then left in the bath for 30 min until the foam was rigid. This cyclic irradiation was established by initial experimentation as sufficient to induce changes in the foam structure without causing collapse.

The basic procedure is summarized as follows: 1. a measured amount of reactant was placed in the container located at a certain distance from the sonotrode; 2. the process was initiated by addition of water (the chemical blowing agent and catalyst for the reaction); 3. ultrasound was applied; 4. on completion of the reaction, the foam was left to cure for 48 h; 5. once the sonicated foams were fully cured, they were de-moulded and cut in half with a coarse-tooth saw and the cross-sections scanned for further analysis.

3.2. Sonication field

The propagation pattern for the ultrasonic field used in this study (for constant values of temperature) is determined by the internal geometry of the water bath, the relative position container–transducer, and by the attenuating properties of the transmitting medium – water. The ultrasonic signal within the bath was mapped with a needle-type hydrophone (Brüel&Kjær, Denmark, type 8103) shielded with a barrier made of the same open-vessel material for representative values. It was connected to a pre-amplifier and a data-logger digital oscilloscope to allow assessment of attenuation and local signal strength during the irradiation process. The signal magnitude (in mV) was recorded at different points within the bath for each of the experimental frequencies (i.e. 20, 25 and 30 kHz) and applied powers. These values were converted thereafter into acoustic pressure values (in Pa) using the voltage sensitivity of the hydrophone. Measurements were taken with increasing distance from the transducer-tip, and at a depth equal to the horizontal plane at which the central part of the foam container was located.

The ultrasound signal attenuates (i.e. reduces in amplitude) as it progresses through the water [22] due to viscous loss. Consequently, the intensity of the ultrasound signal will vary from point to point within the bath. Data extracted from the mapping results showed the decreasing trend as well as partial maxima of pressure values appearing at odd multiples (i.e. 1, 3, 5, 7) of a half-wavelength [23] predicted by the sine propagation wave.

The mapping results of the water bath for the sonotrode irradiating at 20 kHz and 75 W of nominal power (located at 5 cm distance from the bath wall) can be seen in Fig. 3. In the same way, acoustic pressure profiles were produced for all working frequencies and applied powers. These values were used to correlate the impact of signal magnitude to foam porosity.

3.3. Quantifying porosity in polyurethane foams

The bulk density (volume divided by mass) of a foam is indicative of a material's porosity. Therefore, porosity is defined as the fraction of the total volume which is non-occupied, i.e. constructed by voids. To a good approxima-

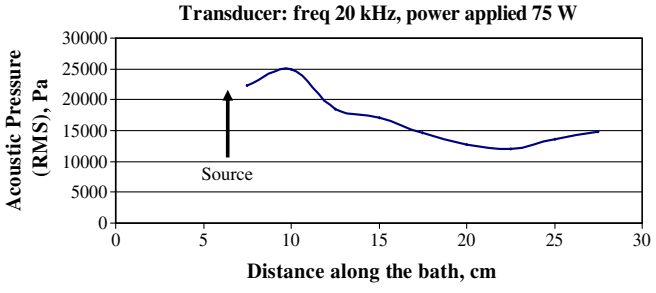

Fig. 3. Acoustic pressure decay within the water bath for applied power to transducer 75 W and 20 kHz frequency.

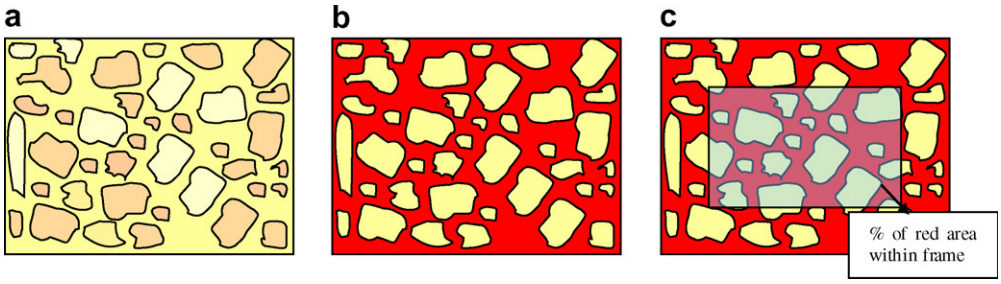

Fig. 4. Software-aided procedure for porosity calculation. (a) Schematic of foam cross-section (b) masking agent to enhance cells walls; and (c) frame for calculation of area fraction.

tion, changes in a foam bulk density are indicative of changes in porosity. Since the mass will be proportional to the volume of material, bulk density will be directly related to the volume fraction of a foam: $\theta = V_p/V_m$, where θ is porosity, V_p volume of pores and V_m volume of material.

To assess the effects of the ultrasound exposure on the foam's cellular structure, a method of characterising the porosity distribution within a material is essential. For open-cell structures (e.g. flexible foams, rocks), porosity can be measured using liquid displacement techniques (e.g. Arquimedes', toluene infiltration displacement, mercury-porosimetry), which provide an average density value for the bulk material (e.g. measurement permeability and tortuosity in a sample). However, for this work, closed-pore foams were manufactured and these methods were not applicable. Instead, each sample was sliced and the porosity assessed using digital image analysis.

Within the sliced samples, the 3D network of the foam structure can be clearly observed (Fig. 1a and 1b) because of the differences in colour between the sectioned walls and the darker recesses of the cells. In order to ensure a more accurate estimation of these areas (i.e. avoid insufficient variation in colour between the sectioned walls and cavity (Fig. 4a)), the contrast between cell walls and cavity was improved. A red masking agent was applied to the surface of the cutting plane prior to scanning the samples (Fig. 4b) effectively isolating the cellular voids. The stained samples were scanned at 1500 dpi resolution in an EPSON Perfection Scanner 1640 SU. These images were then analysed with the Aquinto ('a4i Docu' v.5.0.0) software (Fig. 4c) which calculated the area fraction of the pores by summing the number of red pixels within a region. The frames were centred on horizontal plane of the source and encompassed the exposed volume of foam. Wall and base of the foam were excluded because in these areas local boundary effects influenced the porosity. Similarly, the portion of foam that was produced above the water bath was also excluded. This was the value used to quantify density for each foam in the following sections. Its inverse value will represent the porosity.

4. Results

This section describes the results of two series of experiments to investigate: 1. *porosity as a function of applied*

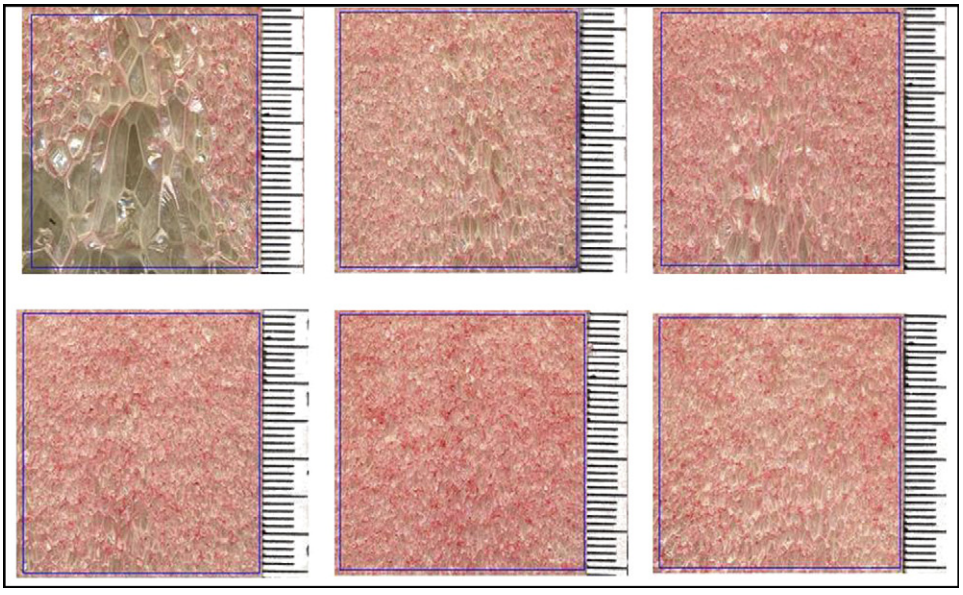

Fig. 5. Selected frames of foams sonicated at 20 kHz and 75 W of applied power to the transducer.

power for a given frequency: the acoustic pressure from each applied power 'seen' by the sample was varied by placing the vessel at different locations in the bath. The corresponding pressure was determined by the signal magnitude map at distances 7.4, 11.1, 12.95, 14.80, 16.65 and 20.35 cm from the ultrasonic probe; and 2. *porosity as a function of frequency* (working frequencies 20, 25 and 30 kHz) *for equal acoustic pressure*. In order to study porosity as a function of frequency, the location of the vessel was fixed at the frequency's first half-wavelength distance external to the vessel axis, tuning the applied powers onto sonotrode in a way that the same wave amplitude was obtained in each case.

4.1. Porosity as a function of applied power for a given frequency

The area fraction (Fig. 5) of the core of the foams (i.e. ±1.5 cm around the axial plane of sonication, e.g. depth of transducer's tip) sonicated at 7.4, 11.1, 12.95, 14.80, 16.65 and 20.35 cm distant from the probe (irradiation conditions: frequency, 20 kHz, applied power 75 W), was used to characterise the porosity of each sample. Plotting these values against measured pressure amplitude at each sample location (Fig. 3) a linear relationship can be observed (Fig. 6). The procedure was repeated using an applied power of 150 W from the transducer for the same frequency. Again, the porosity values from the image analysis were correlated with the measured acoustic pressure at each location and plotted in Fig. 7. Likewise, the porosity values from the image analysis were plotted against pressure at each location along the bath for 25 and 30 kHz frequency and applied powers of 67and 55 W, respectively. Figs. 8 and 9 present the results of those correspondences.

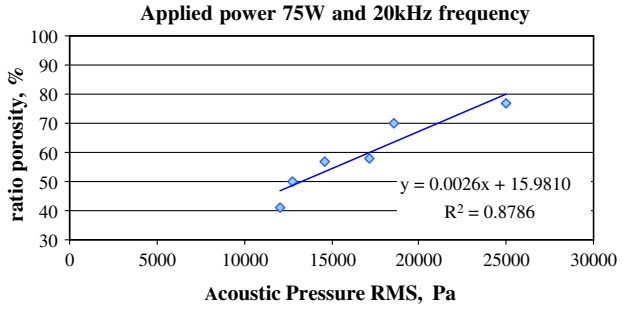

Fig. 6. Percentage porosity for samples irradiated with applied power 75 W and 20 kHz frequency. Acoustic pressure as measured in RMS by hydrophone.

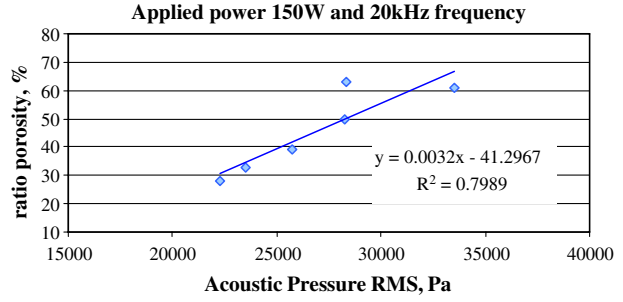

Fig. 7. Percentage porosity for samples irradiated with applied power 150 W and 20 kHz frequency.

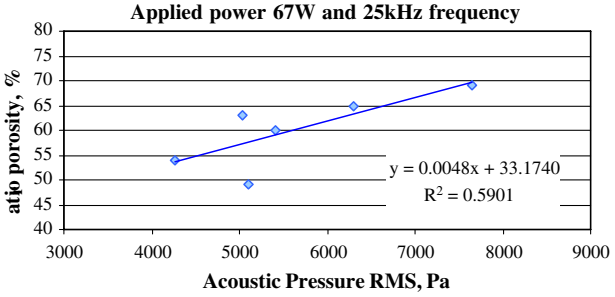

Fig. 8. Percentage porosity for samples irradiated with applied power 67 W and 25 kHz frequency.

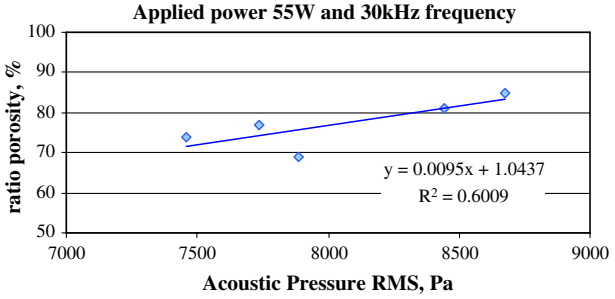

Fig. 9. Percentage porosity for samples irradiated with applied power 55 W and 30 kHz frequency.

4.2. Porosity as a function of frequency for equal acoustic pressure

The selected power applied to the transducer for this series of experiments was tuned in order to obtain an equal value of acoustic pressure (i.e. signal magnitude) when the distance was each frequency's first half-wavelength distance external to the vessel. The acoustic pressure was 8750 Pa (7% tolerance) for 20 kHz located at 11.1 cm from the transducer; for 25 kHz at 8.85 cm; and for 30 kHz at 7.35 cm. Values of porosity versus frequency are plotted in Fig. 10.

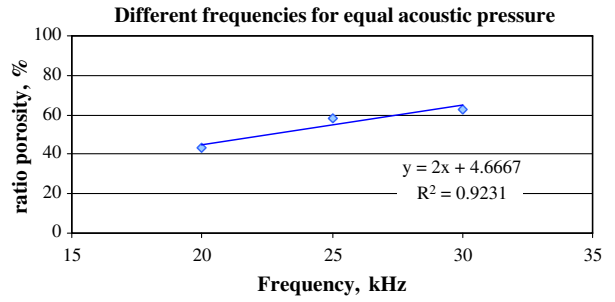

Fig. 10. Percentage porosity of samples irradiated at same acoustic pressure and different frequencies.

5. Discussion

The application of this new technology allows the manufacture of materials with a controlled cellular structure. In this work, polyurethane foams have been irradiated with ultrasound to produce a gradation of porosity. Areas of higher porosity in foams were caused by the formation of larger pores when the mixture was still of a viscoelastic nature (i.e. liquid to solid transition). The authors believe that frequency, applied power and signal magnitude in the bath produced stable cavitation (i.e. rectified diffusion of gas content from the polymer matrix into the cavities) for the water vapour/CO_2 gas filled bubbles. As Leighton refers [24], in a stable cavitation scenario, it can be assumed that the energy stored during the positive half of each stress cycle is not dramatically different from the energy given up during the negative half, therefore experimental conditions of sonication were favourable to the diffusion of gas into the bubble that underwent an incremental but sustainable growth. In addition, a lower value of viscosity was maintained for longer periods of time, hence delaying the viscoelastic stresses that could suppress the stretching motion in latter stages of foam formation. The effect is visible in the foam sample images: a wall thinning effect is distinguishable in those areas where the ultrasound was applied (Fig. 1a and 1b).

The geometry of the water bath and relative positions sonotrode-to-container had an important influence on the acoustic field irradiated in the bath, and hence the acoustic pressure the samples were subjected to. The mapping of the acoustic pressure was relevant at the experiment design stage as it predicted the acoustic signal magnitude of the sonicating field within the bath. If the acoustic intensity produced within was too large in the position at which the polymeric foam was held, transient cavitation effects occurred (i.e. bubbles grew rapidly to a non-equilibrium size and they imploded provoking polymeric cellular collapse through breaking the polymer chains). For this work, experimental conditions were controlled in a way that the acoustic intensity was below the threshold value of transient cavitation and foam growth was pursued.

The lower limit of stable cavitation for this polymeric foam formation was explored by increasing the acoustic pressure until an effect was visible in the foam porosity. From that point, bubble enlargement was proportional to the increment of acoustic pressure. When acoustic intensity reached greater values, but still within the boundaries of stable cavitation, a homogenisation effect in the matrix could be observed after ultrasonic irradiation. This can be explained in terms of the enhanced diffusivity produced: acoustic conditions would be favourable to the nucleation of many bubbles that would be competing for the limited amount of gas available in the matrix during the chemical reaction. The presence of nearby bubbles prevented each one from growing any larger. Bubbles solidified producing an even cellular structure in the final foam. Pores had a smaller size in average (with smaller standard deviation in its distribution). This effect is considered by the authors as a prior step before approaching transient cavitation conditions.

When considering foams subjected to equal value of sound pressure, the effect in the porosity was studied for different values of frequency. As the frequency increased, the bubbles expanded more and had less time to recover its initial size in each cycle. These short periods of expansion produced a larger final volume of bubbles which solidified into pores. Despite the limited number of frequencies that could be tested, results from 20, 25 and 30 kHz frequency of irradiation showed a direct relationship confirming this statement.

6. Conclusions

Precisely controlled, localised application of ultrasound influenced the cellular structure of foamed material in a predictable manner. Our experiments have shown that ultrasound can be used to affect local physical and chemical processes in the foaming medium. It is believed that the cause is a combination of different phenomena: the excitation of bubble nucleation, interference with the polymerisation processes, generation of local pressure changes in the fluid which produces local membrane perturbation, rectified diffusion (i.e. stable cavitation) and enhanced transport of mass through the cell walls. These effects can be observed directly in cross-sections of foam that have been sonicated using the immersion technique during their formation (Fig. 1b).

Future work will investigate the mechanisms underlying the reported effect. This will allow a finer adjustment of ultrasonic radiation conditions and the possibility of extrapolating this application to foaming materials that can be used in specific applications where a tailor-made cellular structure is required '*ad hoc*' (e.g. bio-mimetics and orthopaedics; structural components, etc.).

References

[1] S.J. Kalita, S. Bose, H.L. Hosick, A. Bandyopadhyay, Development of controlled porosity polymer–ceramic composite scaffolds via fused deposition modeling, Materials Science and Engineering Part C 23 (5) (2003) 611–620.

[2] J.M. Taboas, R.D. Maddox, P.H. Krebsbach, S.J. Hollister, Indirect solid free form fabrication of local and global porous, biomimetic and composite 3D polymer–ceramic scaffolds, Biomaterials 24 (1) (2003) 181–194.

[3] Y. Yan, Z. Xiong, Y. Hu, S. Wang, R. Zhang, C. Zhang, Layered manufacturing of tissue engineering scaffolds via multi-nozzle deposition, Materials Letters 57 (18) (2003) 2623–2628.

[4] V.A. Yakushin, N.P. Zhmud, U.K. Stirna, Physicomechanical characteristics of spray-on rigid polyurethane foams at normal and low temperatures, Mechanics of Composite Materials 38 (3) (2002) 273–280.

[5] H.X. Peng, Z. Fan, J.R.G. Evans, J.J.C. Busfield, Microstructure of ceramic foams, Journal of the European Ceramic Society 20 (7) (2000) 807–813.

[6] T.G. van Tienen, R.G.J.C. Heijkants, P. Buma, J.H. de Groot, A.J. Pennings, R.P.H. Veth, Tissue ingrowth and degradation of two biodegradable porous polymers with different porosities and pore sizes, Biomaterials 23 (8) (2002) 1731–1738.

[7] S. Morvan, MMA-Rep, A Representation for Multi-Material Solids, The Graduate School of Clemson University, 2001.
[8] X.D. Zhang, C.W. Macosko, H.T. Davis, A.D. Nikolov, D.T. Wasan, Role of silicone surfactant in flexible polyurethane foam, Journal of Colloid and Interface Science 215 (2) (1999) 270–279.
[9] A.J. Rojas, J.H. Marciano, R.J. Williams, Rigid polyurethane foams: a model of the foaming process, Polymer Engineering and Science 22 (13) (1982) 840–844.
[10] R. Font, M.C. Sabater, M.A. Martínez, The leaching kinetics of acetone in an acetone–polyurethane adhesive waste, Journal of Applied Polymer Science 85 (9) (2002) 1945–1955.
[11] G.J. Price, E.J. Lenz, C.W.G. Ansell, The effect of high intensity ultrasound on the synthesis of some polyurethanes, European Polymer Journal 38 (8) (2002) 1531–1536.
[12] G.J. Price, Ultrasonically enhanced polymer synthesis, Ultrasonics Sonochemistry 3 (3) (1996) S229–S238.
[13] W.J. Cho, H. Park, J.R. Youn, Ultrasonic bubble nucleation in reaction injection moulding of polyurethane, Proceedings of the Institution of Mechanical Engineers, Part B 208 (B2) (1994) 121–128.
[14] J.A. Gallego-Juárez, G. Rodríguez-Corral, E. Riera-Franco De Sarabia, C. Campos-Pozuelo, F. Vázquez-Martínez, V.M. Acosta-Aparicio, Macrosonic system for industrial processing, Ultrasonics 38 (1) (2000) 331–336.
[15] J.A. Gallego-Juárez, G. Rodríguez-Corral, E. Riera-Franco de Sarabia, F. Vázquez-Martínez, V.M. Acosta-Aparicio, C. Campos-Pozuelo. Development of industrial models of high-power stepped-plate sonic and ultrasonic transducers for use in fluids, in: Proceedings of the IEEE Ultrasonics Symposium, 2001.
[16] A. Mulet, J.A. Cárcel, N. Sanjuán, J. Bon, New food drying technologies – use of ultrasound, Food Science and Technology International 9 (3) (2003) 215–221.
[17] W.G. Pitt, Defining the role of ultrasound in drug delivery, American Journal of Drug Delivery 1 (1) (2003) 27–42.
[18] I. Masselin, X. Chasseray, L. Durand-Bourlier, J.M. Laine, P.Y. Syzaret, D. Lemordant, Effect of sonication on polymeric membranes, Journal of Membrane Science 181 (2) (2001) 213–220.
[19] T.G. Leighton, Bubble population phenomena in acoustic cavitation, Ultrasonics Sonochemistry 2 (2) (1995) S123–S136.
[20] J.D. Floros, H. Liang, Acoustically assisted diffusion through membranes and biomaterials, Food Technology 48 (12) (1994) 79–84.
[21] J.D.N. Cheeke, Fundamentals and Applications of Ultrasonic Waves, first ed., CRC Press, Boca Raton, FL, 2002, ISBN 084930130-0 (p. 480).
[22] J. Blitz, Fundamentals of Ultrasonics, second ed., Butterworths, London, 1967, 214 pages.
[23] P.M. Kanthale, P.R. Gogate, A.B. Pandit, A. Marie Wilhelm, Mapping of an ultrasonic horn: link primary and secondary effects of ultrasound, Ultrasonics Sonochemistry 10 (6) (2003) 331–335.
[24] T.G. Leighton, The Acoustic Bubble, first ed., Academic Press, San Diego, CA, 1994.